FEBS Letters 505 (2001) 436–440 FEBS 25264

Stability and DNA-binding properties of the ω regulator protein from the broad-host range *Streptococcus pyogenes* plasmid pSM19035

Rolf Misselwitz[a], Ana B. de la Hoz[b], Silvia Ayora[b], Karin Welfle[a], Joachim Behlke[a], Kazutaka Murayama[c], Wolfram Saenger[c], Juan C. Alonso[b], Heinz Welfle[a,*]

[a] *Max-Delbrück-Centrum für Molekulare Medizin, D-13092 Berlin, Germany*
[b] *Departamento de Biotecnología Microbiana, Centro Nacional de Biotecnología, C.S.I.C., E-28049 Madrid, Spain*
[c] *Institut für Kristallographie, Freie Universität Berlin, D-14195 Berlin, Germany*

Received 28 July 2001; accepted 27 August 2001

First published online 6 September 2001

Edited by Pierre Jolles

Abstract At the transcriptional level, the pSM19035-encoded ω protein coordinates the expression of proteins required for control of copy number and maintenance of plasmids. Using circular dichroism, fluorescence spectroscopy, ultracentrifugation and an electrophoretic mobility shift assay, the wild-type ω protein and a variant with a C-terminal hexa-histidine tag (ω-H_6) were characterized. The ω protein is mainly α-helical (42%), occurs as homodimer in solution, unfolds thermally with half transition temperatures, T_m, between ~43 and ~78°C depending on the ionic strength of the buffer, and binds *P*copS-DNA with high affinity. The ω-H_6 protein has a modified conformation with lower α-helix content (29%), lower thermal stability, and strongly reduced affinity to *P*copS-DNA.

Key words: Plasmid copy number control; Transcriptional repressor; Protein–DNA interaction; Protein stability; Circular dichroism; Fluorescence; Thermal unfolding; Urea unfolding

1. Introduction

The low-copy-number, broad-host-range and non-conjugative *Streptococcus pyogenes* plasmid pSM19035 shares >90% identity with the other members of the *inc18* incompatibility group (namely the conjugative plasmids pIP501 and pAMβ1) in regions associated with replication (*cop*, RNAIII, *rep*, *ori*) and maintenance of plasmid copy-number stability [segA (αβγ) and segB (δω and ωεζ)] [1–6]. pSM19035-encoded ω protein binds specifically, with high cooperativity and with similar affinity to the upstream promoter regions of three genes and directly represses their transcription: δ (*P*δ), ω (*P*ω) and *cop*S (*P*cop; contains two overlapping promoters *P*cop1 and *P*cop2); ω protein indirectly controls expression of the ε and ζ genes of the ω-ε-ζ operon [7]. Inhibition of transcription by ω protein does not occlude the binding of vegetative *Bacillus subtilis* RNA polymerase (σ^ARNAP) to the *P*δ, *P*ω and *P*cop promoters [7].

Because ω protein has a central role in regulating plasmid replication and stable maintenance functions [5–7], a detailed analysis of its properties was undertaken. Crystals of ω protein diffracting to 1.5 Å resolution were grown [8] and their structure was determined by X-ray analysis. ω Protein belongs to the MetJ/Arc repressors superfamily featuring a dimer with a ribbon-helix-helix DNA-binding motif, and model building suggests that the β-ribbon is located in the major groove of the DNA substrate (K.M., Peter Orth, A.B.d.l.H., J.C.A. and W.S., submitted). Here, we describe the thermal- and urea-induced unfolding behavior of ω protein and of an ω variant containing a C-terminal hexa-histidine tag (ω-H_6). This variant protein was constructed to facilitate the preparation of ω protein, but proved not to be suitable for further studies because of the influence of the His tag on conformation and unfolding behavior of ω-H_6 protein and its strongly reduced binding affinity to DNA fragments containing upstream promoter sequences of δ, ω and *cop*S genes.

2. Materials and methods

2.1. Bacterial strains and plasmids

Escherichia coli BL21(DE3) strain, pCB230, pT712-borne ω (pT712ω) and pT712-borne mutant ω-H_6 gene, were as previously described [7–9].

2.2. Chemicals, DNA, RNA, enzymes, proteins and reagents

Urea (ultrapure) from ICN Biomedicals, Eschwege, Germany, was used without further purification. All other chemicals were purchased from Merck, Darmstadt, Germany, in p.a. quality. DNA restriction and modification enzymes, ATP, RNaseA, and poly[d(I-C)] were purchased from Boehringer Mannheim, Germany.

The concentrations of dsDNA were determined using a molar extinction coefficient per nucleotide of 6500/M/cm at 260 nm.

The ω and ω-H_6 proteins were prepared from BL21(DE3) cells carrying pT712ω or pT712ω-H_6 after induction with IPTG (1 mM) during 30 min and addition of rifampicin (200 μg/ml) during 90 min. Cells were resuspended in buffer A (50 mM Tris–HCl, pH 7.5, 10 mM $MgCl_2$, 2 mM DTE, 0.2 mM PMSF, 5% glycerol) containing 50 mM NaCl and lysed with a French press. The crude extract was centrifuged at $12\,000 \times g$ for 30 min and the supernatant was used for further purification by conventional column chromatography (phosphocellulose, S-Sepharose and Superose 12). The ω-H_6 protein was purified using a nickel-chelating column (Applied Biosystems, Weiterstadt, Germany). The protein concentrations were determined at 276 nm using absorption coefficients of $A_{1\%,1cm} = 3.63$ and $A_{1\%,1cm} = 3.29$ for ω and ω-H_6 proteins, respectively, as calculated from the amino acid composition according to ([10]; http://www.expasy.ch/tools/protparam.html). The molecular masses of the ω and ω-H_6 protein monomers calculated from the sequence are 7988 and 8811 Da, respectively, and theoretical isoelectric points of both proteins are 9.5.

2.3. Circular dichroism (CD) and fluorescence measurements

CD spectra in the far ultraviolet (UV) region were obtained with a Jasco-J720 spectropolarimeter using 0.01, 0.1 and 1 cm path length

*Corresponding author. Fax: (49)-30-94062840.
E-mail address: welfle@mdc-berlin.de (H. Welfle).

PII: S0014-5793(01)02865-4

quartz cuvettes in a thermostated cell holder at 25 ± 0.2°C. Protein concentrations ranged from 0.01 to 0.9 mg/ml in buffer B (50 mM sodium phosphate, pH 7.5) or buffer C (50 mM Tris–HCl, pH 7.5) with 0–3 M NaCl. Molar mean residue ellipticities (Θ) (deg/cm^2/dmol) were calculated using mean residue molecular masses of 112.5 for ω and 114.4 for ω-H_6. The content of secondary structure was determined from the far UV CD spectra using the variable selection method (program VARSLC1) starting with a set of 33 reference proteins [11]. In parallel, the secondary structure was predicted from the amino acid sequence using the PHDsec program of the PredictProtein package ([12,13]; http://cubic.bioc.columbia.edu/predictprotein).

ω Protein contains no tryptophan, but two tyrosines per monomer, Tyr62 and Tyr66. Tyrosine fluorescence spectra were obtained with a Shimadzu RF5001 spectrofluorimeter at an excitation wavelength of 276 nm, and 5- and 10-nm bandwidths for excitation and emission monochromators, respectively. Proteins at concentrations of 0.09 mg/ml were in buffer B, 150 mM NaCl.

2.4. Urea- and thermal-induced unfolding

Urea-induced unfolding was monitored by changes of Θ at 222 nm and by changes of the intensity at the maximum of the tyrosine fluorescence, 302 nm. For unfolding experiments, ω and ω-H_6 proteins (0.01 or 0.09 mg/ml) were incubated overnight at 20°C with the respective buffer and urea conditions. For refolding experiments, ω protein (0.4 mg/ml) was first unfolded by overnight incubation in buffer B, 150 mM NaCl, 5 M urea. Individual samples (0.09 mg/ml ω protein in buffer B containing 150 mM NaCl and the desired urea concentration) were prepared by mixing appropriate aliquots of protein stock solution, urea-free buffer B and buffer B containing 5 M urea, and then incubated for about 15 h at 20°C. For thermal unfolding of ω and ω-H_6 proteins, the temperature was increased to 90°C at a heating rate of 20°C/h, and changes in Θ were monitored at 222 nm. The reversibility of unfolding of the proteins was checked by cooling (40°C/h) to 15 or 20°C. The fraction f_u of unfolded protein was calculated from the urea unfolding curves according to the following equation:

$$f_u = \frac{F_u - F_{obs}}{F_n - F_u} \quad (1)$$

where F_n and F_u are Θ or fluorescence intensity of the native and unfolded protein, respectively, and F_{obs} is the Θ or fluorescence intensity at the respective urea concentration [14].

2.5. Analytical ultracentrifugation

Molecular-mass studies on ω protein were performed in an XL-A-type analytical ultracentrifuge (Beckman, Palo Alto, CA, USA) equipped with UV absorbance optics. Sedimentation equilibrium distribution was analyzed using externally loaded six-channel centerpieces of 12-mm path length with the capacity to handle three solvent solution pairs of about 70 μl of liquid; buffer B, 0.15 M NaCl, was used as solvent. In order to determine the state of oligomerization of ω protein and the equilibrium constant, a broad range of protein concentrations from 0.07 to 1.01 mg/ml were analyzed. Sedimentation equilibrium was reached after 2 h of overspeed at 24 000 rpm, followed by an equilibrium speed of 20 000 rpm for 24–28 h at 10°C. The radial absorbance in each compartment was scanned at three different wavelengths between 230 and 280 nm, selected appropriately depending on the loading concentration. Molecular-mass calculations employed the simultaneous fitting of the experimental radial absorbance distribution curves described by

$$A_r = A_{r_m} \exp[MK(r^2 - r_m^2)] \quad (2)$$

with

$$K = \frac{[(1-\rho\bar{v})\omega^2]}{2RT} \quad (3)$$

using our program Polymole [15]. In these equations, A_r and A_{r_m} are the radial absorbance at radius r and at meniscus position r_m, respectively; M is the molar mass, ρ the solvent density, $\bar{v}$ the partial specific volume, ω the angular velocity, R the gas constant, and T the absolute temperature. The program Polymole [15] allows the determination of partial concentrations and equilibrium constants of self-associating proteins. The experimental data obtained for the ω protein were examined assuming a monomer–dimer equilibrium.

2.6. Measurement of protein–DNA interactions

Electrophoretic mobility shift assays (EMSA) were performed with gel-purified 291-bp ^{32}P-end-labelled DNA containing the *P*copS promoter binding site (0.2 nM). The DNA fragments were incubated for 15 min at the indicated temperatures in a 20-μl final volume of buffer C, 10 mM $MgCl_2$, 50 mM NaCl, with different amounts of ω protein in the presence of 1 μg of poly[d(I-C)] as non-specific-competitor DNA, as previously described [7]. The mixture was then loaded and separated on a 4% non-denaturing polyacrylamide gel electrophoresis run with 45 mM Tris-borate, pH 8.0, 10 mM EDTA, at 50 V and 4°C and dried prior to autoradiography.

3. Results

3.1. Purification of the pSM19035 ω and ω-H_6 proteins

The ω and ω-H_6 proteins were overexpressed using the T7 RNA polymerase expression system (see [7]). Plasmids pT712ω and pT712ω-H_6, which contain genes ω and ω-H_6 downstream of a T7 promoter, were introduced into *E. coli* strain BL21(DE3)/pLysS, and genes of ω and ω-H_6 proteins were overexpressed by the addition of IPTG and rifampicin, as previously described [7]. Under the expression and preparation conditions described in Section 2, the ω and ω-H_6 proteins account for ∼4% and ∼6%, respectively, of total protein mass, and yields of about 1 and 1.5 mg, respectively, per liter of induced culture were obtained.

3.2. Spectroscopic characterization of ω and ω-H_6 proteins

General spectroscopic features of the far UV CD spectra of ω and ω-H_6 proteins are similar and point to mostly α-helical structures of both proteins (Fig. 1A). In buffer B without NaCl, at protein concentrations of 0.9 mg/ml and in 0.01-cm cuvettes, spectra can be measured up to 180 nm and are characterized by maxima at 190 nm, and double minima at 208 and 222 nm. A small blue shift of the zero transition point (200.0 and 198.5 nm for ω and ω-H_6 protein, respectively) and lower Θ values of the spectrum of ω-H_6 in comparison to ω protein indicate differences in the conformations of the two proteins. In the absence of NaCl, the content of α-helices is significantly higher for ω protein (42%) than for ω-H_6 protein (29%), but the differences in the content of β-sheets (13% versus 18% for ω and ω-H_6 proteins, respectively) and turns (19% versus 22% for ω and ω-H_6 proteins, respectively) are smaller, as calculated by VARSLC1. The secondary structure of ω protein is not affected by the ionic strengths of the buffer. The CD spectra of ω protein in buffer B containing 0.15–3 M NaCl are practically identical between 195 and 260 nm with the CD spectrum in buffer B without NaCl, as shown in Fig. 1A. The amounts of secondary structure calculated from the CD spectrum agree with those calculated against full-length ω protein (42% α-helix, 7% β-sheet, 51% others) from the X-ray crystal structure, where only amino acids 23–71 are clearly seen in the electron density map and amino acids 1–22 are disordered (K.M., Peter Orth, A.B.d.l.H., J.C.A. and W.S., ibid.).

Using the PHDsec program [12,13], the secondary structure of ω protein was predicted from the amino acid sequence to be 23.9% α-helix, 7.0% β-sheet and 69% loop structures (all residues not in α-helices or β-sheets). These values changed to 23.9% α-helix, 4.2% β-sheet and 32.4% loop structures when only values with an expected average accuracy >82% (reliability index >5) were considered; under these stringent conditions, for 39% of the residues, no prediction was given. For both reliability indices, only one α-helix was predicted for the

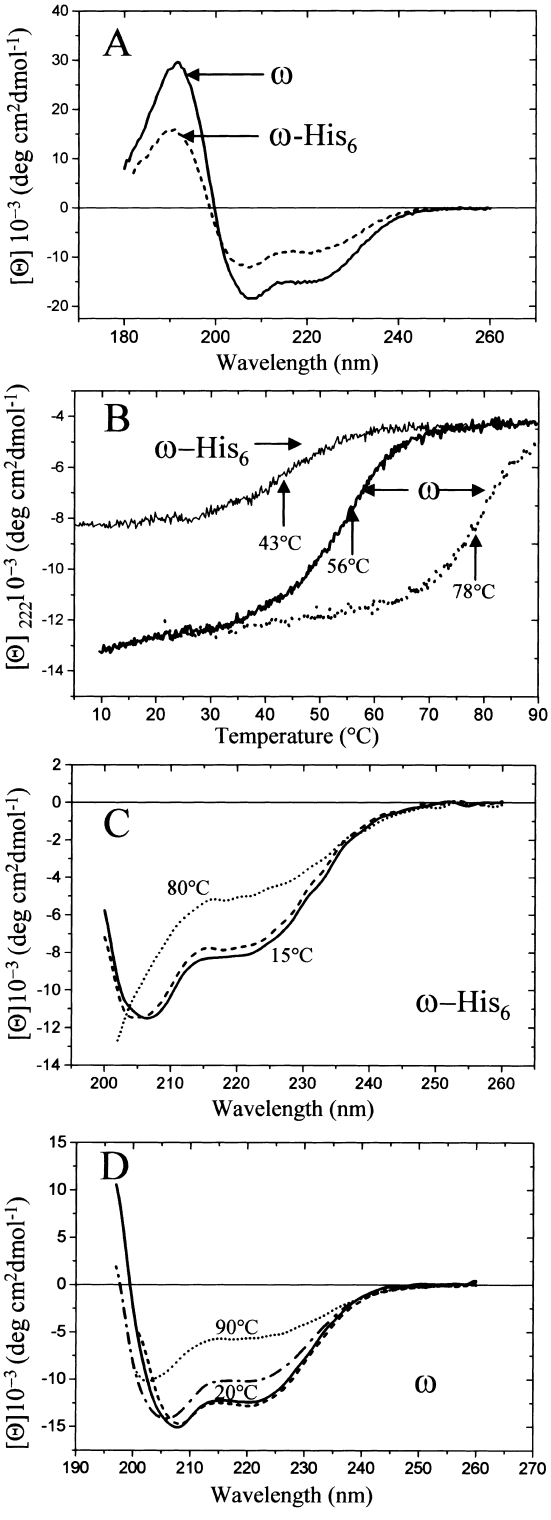

Fig. 1. Far UV CD spectra, thermal stability and refolding of ω and ω-H_6 proteins. A: CD spectra of ω protein (solid line) and ω-H_6 protein (dashed line) in buffer B without NaCl. B: Melting curves of ω-H_6 (thin solid line) and ω protein (thick solid line) in buffer B, 150 mM NaCl, and melting curve of ω protein in buffer B, 3 M NaCl (dotted line), monitoring changes of Θ at 222 nm. C: CD spectra of ω-H_6 protein in buffer B, 150 mM NaCl, in the peptide region between 200 and 260 nm measured at 15°C before heating (solid line), at 80°C (dotted line), and after cooling to 15°C (dashed line). D: CD spectra of ω protein in buffer C measured at 20°C (solid line), at 90°C (dotted line), and after cooling to 20°C (dash-dotted line); and in buffer C, 3 M NaCl, after cooling to 20°C (dashed line).

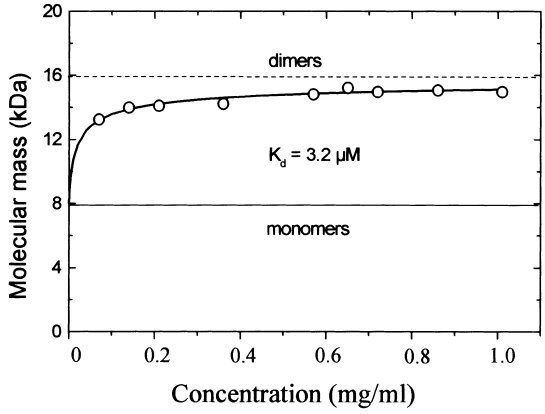

Fig. 2. Sedimentation equilibrium measurements of ω protein. Plot of molecular mass versus ω protein concentration. The dashed and solid horizontal lines indicate the theoretical molecular masses of dimer and monomer, respectively. The solid curve was calculated assuming a monomer–dimer equilibrium and yields a dissociation constant $K_d = 3.2$ μM.

amino acid region 52–68. This was confirmed by the X-ray crystal structure analysis (helix B starts at Val51 and terminates at Tyr66), but an additional helix A comprising amino acids Ala34 to Asn47 was identified in the crystal structure (K.M., Peter Orth, A.B.d.l.H., J.C.A. and W.S., ibid.), but not predicted.

3.3. ω Protein is a dimer in solution

Sedimentation equilibrium experiments were performed in the ω protein concentration range 0.07–1.01 mg/ml. In some experiments, small amounts ($< 5\%$) of high-molecular-mass aggregates were observed near the cell base. To obtain reliable fitting results, it is mandatory to eliminate data points corresponding to these aggregates. Simultaneous fitting of the radial absorbance distributions using the program Polymole [15] resulted in molecular-mass values between 13.2 kDa ($c = 0.07$ mg/ml) and 15 kDa ($c = 1.01$ mg/ml). The data correspond to a monomer–dimer equilibrium with an average equilibrium dissociation constant $K_d = 3.2$ μM (Fig. 2).

3.4. Thermal stability of ω and ω-H_6 proteins

Thermal unfolding of ω and ω-H_6 proteins in buffer B containing up to 3 M NaCl was monitored by changes of the Θ at 222 nm. Protein concentrations and heating rates were 0.09 mg/ml and 20°C/h, respectively. In Fig. 1B, melting curves of ω and ω-His_6 proteins are shown. Half-transition temperatures, T_m, were obtained by calculating the first derivative of the melting curves. At 0.15 M NaCl, the ω-H_6 and ω proteins unfold with T_m values of 43 and 56°C, respectively. With increasing ionic strength, the thermostability of ω protein increases to a T_m value of 78°C at 3 M NaCl (Fig. 1B, dotted line). There is no obvious evidence for intermediates during thermal unfolding.

The reversibility of thermal-induced unfolding of ω-H_6 (Fig. 1C) and ω proteins (Fig. 1D) was checked by slow cooling. At 0.15 M NaCl, ω-H_6 protein refolds nearly completely (Fig. 1C, compare solid with dashed line), whereas ω protein only partially refolds at this ionic strength (Fig. 1D, dash–dotted line). At 3 M NaCl, however, ω protein also refolds completely, as indicated by the nearly identical CD spectra

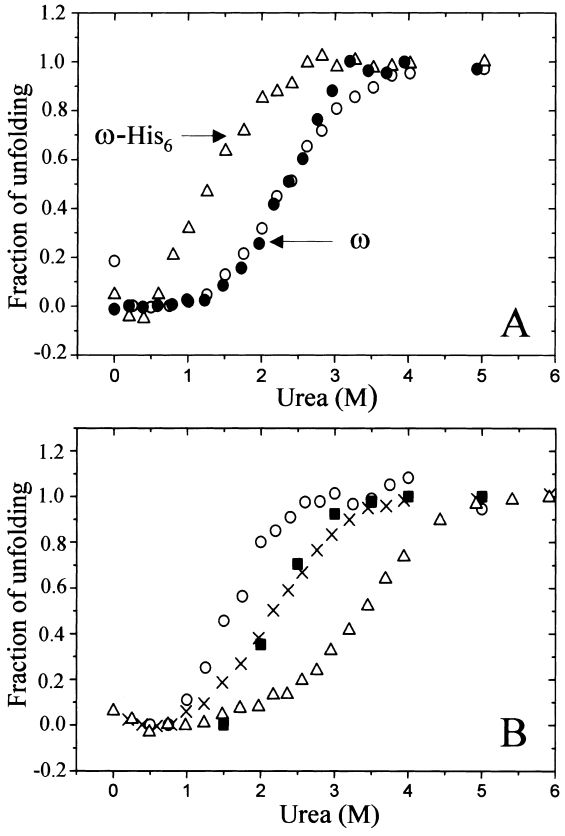

Fig. 3. Protein concentration and ionic strength dependence of urea-induced unfolding of ω and ω-H_6 proteins at 25°C. A: Normalized urea-induced unfolding curves of ω-H_6 protein (triangles) and ω protein (open and closed circles) were calculated from experiments monitoring Θ at 222 nm (triangles and open circles) and changes of the tyrosine fluorescence-emission intensity at 302 nm (closed circles) in buffer B, 0.15 M NaCl, at various urea concentrations and protein concentration of 0.09 mg/ml. B: Unfolding curves calculated from CD experiments of ω protein in buffer B, 0.15 M NaCl, protein concentrations 0.01 mg/ml (circles) and 0.09 mg/ml (crosses), and in buffer B, 1.0 M NaCl, at 0.09 mg/ml (triangles). Refolding of ω protein was studied in buffer B, 0.15 M NaCl, at 0.09 mg/ml (squares).

before heating and after cooling (Fig. 1D, compare solid with dashed line).

3.5. Urea-induced unfolding of ω and ω-H_6 proteins

Spectral probes of unfolding and refolding were Θ at 222 nm and the tyrosine fluorescence emission intensity that reflect changes of secondary and tertiary structure, respectively. Fig. 3A shows the urea-induced normalized unfolding curves of ω protein monitored by CD at 222 nm (open circles) and fluorescence (closed circles), and the unfolding curve of ω-H_6 protein monitored by CD (triangles). The ω and ω-H_6 proteins unfold cooperatively at relatively low urea concentrations with half transition concentrations $c_{1/2}$ of 2.2 and 1.3 M urea, respectively (Fig. 3A). The coincidence of the CD and fluorescence-monitored unfolding curves of ω protein point to a simple two-state transition between folded and unfolded molecules. Evidently, ω-H_6 protein not only differs in its secondary structure (Fig. 1A), but also has a significantly lower thermodynamic stability in comparison to ω protein (Fig. 3A).

Unfolding of ω and ω-H_6 proteins is strongly dependent on protein concentration as expected for oligomeric proteins [16,17]. Fig. 3B shows the unfolding curves of ω protein in buffer B, 0.15 M NaCl, at low (0.01 mg/ml; circles) and high protein concentration (0.09 mg/ml; crosses). Unfolding is characterized by half transition concentrations $c_{1/2}$ of 1.6 M and 2.2 M urea at the lower and higher protein concentration, respectively. Fig. 3B also shows a refolding curve of ω protein measured at 0.09 mg/ml (squares). The data illustrate the reversibility of urea-induced unfolding of ω protein.

The unfolding curves shown in Fig. 3 were evaluated, as described [14], assuming a two-state transition between folded dimers and unfolded monomers [18]. From the data in the transition region, the equilibrium unfolding constants K_u were determined according to

$$K_u = 2P_t \frac{f_u^2}{1-f_u} \quad (4)$$

where P_t is the total protein concentration (in moles of monomer) and f_u is the fraction of unfolding. From the K_u values, the free energies of unfolding, ΔG_u, were calculated using equation

$$\Delta G_u = -RT \ln K_u \quad (5)$$

ΔG_u values vary linearly with urea concentration and were analyzed using the linear extrapolation model

$$\Delta G_u = \Delta G_{u,H_2O} - m[\text{urea}] \quad (6)$$

where m is a measure of the dependence of ΔG_u on urea concentration, and $\Delta G_{u,H_2O}$ is the value obtained by linear extrapolation of the ΔG_u values to 0 M urea. The parameters characterizing the urea denaturation of ω protein are $\Delta G_{u,H_2O}$ = 12.2 kcal/mol and m = −2.53 kcal/mol/K for protein

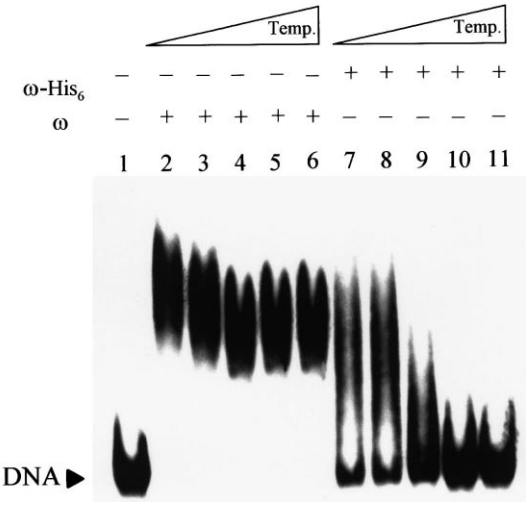

Fig. 4. Efficiency of ω and ω-H_6 proteins binding to *P*copS DNA at different temperatures. ^{32}P-labelled 291-bp *P*copS DNA (0.2 nM) and 1 μg of poly[d(I-C)], as non-specific competitor DNA, were incubated for 15 min with 2.6 μg/ml ω protein (32 nM monomers) and 23 μg/ml ω-H_6 protein (260 nM monomers) in buffer C, 10 mM $MgCl_2$ and 50 mM NaCl, at 4, 10, 20, 30 and 37°C (lanes 2–6, and 7–11). The protein–DNA complexes were analyzed by EMSA. The symbols − and + indicate the absence and presence of protein, respectively.

concentration 0.01 mg/ml, and $\Delta G_{u,H_2O} = 11.1$ kcal/mol and $m = -1.96$ kcal/mol/K for 0.09 mg/ml.

Similar to thermal unfolding, with increasing ionic strength, the stability of ω protein against urea-induced unfolding is enhanced, as indicated by the shift of the unfolding curves to higher denaturant concentrations. As an example, Fig. 3B (triangles) shows an unfolding curve measured in buffer B, 1.0 M NaCl.

3.6. ω-H_6 protein binds to its target site at low temperature

Previously, it has been shown that ω protein binds cooperatively to the promoters of the *cop*S, δ and ω genes. The affinity of ω protein for *P*cop, *P*δ and *P*ω was determined by EMSA and DNase I footprinting [7]. The apparent binding constant ($K_{d,app}$) of ω–*P*copS DNA complex formation at pH 7.5 and 37°C in buffer C, 10 mM $MgCl_2$, 50 mM NaCl, was estimated to be ∼4 nM [7].

Comparable DNA-binding assays were performed for ω-H_6 protein at various temperatures (from 4 to 37°C) with 0.2 nM [^{32}P]*P*copS DNA, 2.6 μg/ml ω protein (32 nM monomers) and 23 μg/ml ω-H_6 protein (260 nM monomers). The EMSA study indicated that the binding affinity of ω-H_6 protein to *P*copS DNA is much weaker than that of ω protein (Fig. 4). At all tested temperatures (4–37°C), 2.6 μg/ml ω protein completely transfer the available *P*copS DNA into the complex, whereas as much as 23 μg/ml ω-H_6 protein are necessary to bind a fraction of DNA at least at low temperatures (4 and 10°C). At 10°C and pH 7.5, the ω-H_6 protein binds to *P*copS DNA with a $K_{d,app}$ of ∼50 nM; the affinity was greater than five-fold reduced when the experiments were performed at 20°C, and no binding was observed at higher temperatures. This we associate with the low thermal stability of ω-H_6 protein whose unfolding starts already at ∼35°C.

4. Discussion

Under the conditions chosen in this study, thermal- or urea-induced unfolding of ω protein is reversible. Urea-induced unfolding monitored by fluorescence and CD spectroscopy revealed similar curves without obvious evidence for the formation of largely populated intermediates, pointing to a two-state mechanism of unfolding. The data, however, can not exclude low populations of folding intermediates which can be expected for the formation of folded dimers from unfolded monomers. The strong protein-concentration dependence of the unfolding suggests that ω protein occurs as oligomer in solution. Our sedimentation equilibrium measurements indicate dimers as the main component of ω protein in 50 mM sodium phosphate, pH 7.5, 150 mM NaCl, at the protein concentration range between 0.07 and 1.0 mg/ml (Fig. 2). This is in contradiction to the finding of ω protein tetramers in an earlier study using gel-filtration chromatography [7], but is supported by the fact that ω protein crystallized as homodimer from 50 mM Tris–HCl, pH 7.5, 50 mM NaCl, 5% glycerol in the presence of the precipitating agent PEG 3350, as shown by the X-ray crystal structure analysis (K.M., Peter Orth, A.B.d.l.H., J.C.A. and W.S., ibid.). The results do not exclude tetramers formed by the association of two dimers in complexes of ω protein with its target DNA [7].

Acknowledgements: We thank Mrs. B. Kannen for technical assistance. A.B.d.l.H. and S.A. were recipients of fellowships of the Gobierno Vasco and Ministerio de Educación, respectively. This work was partially supported by Grants BMC2000-0548 from MCT-DGI and BIO4-CT98-0099 to J.C.A., by Fonds der Chemischen Industrie and EU-Grant BIO4-CT98-0106 to W.S., and by Deutsche Forschungsgemeinschaft to H.W. (GRK 80/2 Partial Project and We1745/5-1) and W.S. (Sa196/38-1).

References

[1] Brantl, S., Behnke, D. and Alonso, J.C. (1990) Nucleic Acids Res. 18, 4783–4789.
[2] Swinfield, T.-J., Oultram, J.D., Thompson, D.E., Brehn, J.K. and Minton, N.P. (1990) Gene 87, 79–90.
[3] Ceglowski, P., Boitsov, A., Chai, S. and Alonso, J.C. (1993) Gene 136, 1–12.
[4] Brantl, S., Kummer, C. and Behnke, D. (1994) Gene 142, 155–156.
[5] del Solar, G. and Espinosa, M. (2000) Mol. Microbiol. 37, 492–500.
[6] Bingle, L.E.H. and Thomas, C.M. (2001) Curr. Opin. Microbiol. 4, 194–200.
[7] de la Hoz, A.B., Ayora, S., Sitkiewicz, I., Fernández, S., Pankiewicz, R., Alonso, J.C. and Ceglowski, P. (2000) Proc. Natl. Acad. Sci. USA 97, 728–733.
[8] Murayama, K., de la Hoz, B.A., Alings, C., Lopez, G., Orth, P., Alonso, J.C. and Saenger, W. (1999) Acta Cryst. D55, 2041–2042.
[9] Studier, F.W. (1991) J. Mol. Biol. 219, 37–44.
[10] Gill, S.C. and von Hippel, P.H. (1989) Anal. Biochem. 182, 319–326.
[11] Johnson Jr., W.C. (1990) Proteins Struct. Funct. Genet. 7, 205–214.
[12] Rost, B. and Sander, C. (1993) J. Mol. Biol. 232, 584–599.
[13] Rost, B. (1996) Methods Enzymol. 266, 525–539.
[14] Pace, C.N. and Scholtz, J.M. (1997) in: Protein Structure: A Practical Approach (Creighton, T.E., Ed.), pp. 299–321, IRL Press, Oxford.
[15] Behlke, J., Ristau, O. and Schönfeld, H.-J. (1997) Biochemistry 36, 5149–5156.
[16] Welfle, H., Misselwitz, R., Welfle, K., Groch, N. and Heinemann, U. (1992) Eur. J. Biochem. 204, 1049–1055.
[17] Neet, K.E. and Timm, D.E. (1994) Protein Sci. 3, 2167–2174.
[18] Welfle, H., Welfle, K., Misselwitz, R., Groch, N. and Heinemann, U. (1993) J. Biomol. Struct. Dyn. 2, 381–394.